

# Association of longitudinal white matter degeneration and cerebrospinal fluid biomarkers of neurodegeneration, inflammation and Alzheimer's disease in late-middle-aged adults

Annie M. Racine<sup>1,2</sup> · Andrew P. Merluzzi<sup>1,2</sup> · Nagesh Adluru<sup>3</sup> · Derek Norton<sup>4</sup> ·  
Rebecca L. Kosciak<sup>5</sup> · Lindsay R. Clark<sup>6,2,5</sup> · Sara E. Berman<sup>2</sup> ·  
Christopher R. Nicholas<sup>6,2</sup> · Sanjay Asthana<sup>6,2</sup> · Andrew L. Alexander<sup>3,7,8</sup> ·  
Kaj Blennow<sup>9,10</sup> · Henrik Zetterberg<sup>9,10,11</sup> · Won Hwa Kim<sup>12,4</sup> · Vikas Singh<sup>2,12,4</sup> ·  
Cynthia M. Carlsson<sup>6,2</sup> · Barbara B. Bendlin<sup>2,5</sup> · Sterling C. Johnson<sup>6,2,5,3</sup>

Published online: 9 June 2017

© Springer Science+Business Media New York 2017

**Abstract** Alzheimer's disease (AD) is characterized by substantial neurodegeneration, including both cortical atrophy and loss of underlying white matter fiber tracts. Understanding longitudinal alterations to white matter may provide new insights into trajectories of brain change in both healthy aging and AD, and fluid biomarkers may be particularly useful in this effort. To examine this, 151 late-middle-aged participants enriched with risk for AD with at least one lumbar puncture and two diffusion tensor imaging (DTI) scans were selected for analysis from two large observational and longitudinally followed cohorts. Cerebrospinal fluid (CSF) was assayed for biomarkers of AD-specific pathology (phosphorylated-tau/A $\beta$ 42 ratio), axonal degeneration

(neurofilament light chain protein, NFL), dendritic degeneration (neurogranin), and inflammation (chitinase-3-like protein 1, YKL-40). Linear mixed effects models were performed to test the hypothesis that biomarkers for AD, neurodegeneration, and inflammation, or two-year change in those biomarkers, would be associated with worse white matter health overall and/or progressively worsening white matter health over time. At baseline in the cingulum, phosphorylated-tau/A $\beta$ 42 was associated with higher mean diffusivity (MD) overall (intercept) and YKL-40 was associated with increases in MD over time. Two-year change in neurogranin was associated with higher mean diffusivity and lower fractional anisotropy overall (intercepts) across white matter in the entire brain

**Electronic supplementary material** The online version of this article (doi:10.1007/s11682-017-9732-9) contains supplementary material, which is available to authorized users.

✉ Sterling C. Johnson  
scj@medicine.wisc.edu

<sup>1</sup> Neuroscience and Public Policy Program, University of Wisconsin, Madison, WI, USA

<sup>2</sup> Alzheimer's Disease Research Center, University of Wisconsin School of Medicine and Public Health, Madison, WI 53705, USA

<sup>3</sup> Waisman Laboratory for Brain Imaging and Behavior, University of Wisconsin-Madison, Madison, WI 53705, USA

<sup>4</sup> Department of Biostatistics and Medical Informatics, University of Wisconsin – Madison, Madison, WI 53792, USA

<sup>5</sup> Wisconsin Alzheimer's Institute, University of Wisconsin School of Medicine and Public Health, Madison, WI 53705, USA

<sup>6</sup> Geriatric Research Education and Clinical Center, William S. Middleton Memorial VA Hospital, 2500 Overlook Terrace, Madison, WI 53705, USA

<sup>7</sup> Department of Medical Physics, University of Wisconsin School of Medicine and Public Health, Madison, WI 53705, USA

<sup>8</sup> Department of Psychiatry, University of Wisconsin School of Medicine and Public Health, Madison, WI 53719, USA

<sup>9</sup> Department of Psychiatry and Neurochemistry, Institute of Neuroscience and Physiology, The Sahlgrenska Academy at the University of Gothenburg, Mölndal, Sweden

<sup>10</sup> Clinical Neurochemistry Laboratory, Sahlgrenska University Hospital, Mölndal, Sweden

<sup>11</sup> Institute of Neurology, University College London, London, UK

<sup>12</sup> Department of Computer Sciences, University of Wisconsin – Madison, Madison, WI 53706, USA

and in the cingulum. These findings suggest that biomarkers for AD, neurodegeneration, and inflammation are potentially important indicators of declining white matter health in a cognitively healthy, late-middle-aged cohort.

**Keywords** Preclinical Alzheimer's disease · Cerebrospinal fluid · White matter · Biomarkers · Longitudinal · Linear mixed effects

### Abbreviations

DTI	Diffusion Tensor Imaging
WRAP	Wisconsin Registry for Alzheimer's Prevention
FA	fractional anisotropy
MD	mean diffusivity
APOE $\epsilon$ 4	apolipoprotein E gene
FH	(parental) family history
WM	white matter
GM	gray matter
FSL	FMRIB Software Library
ANTS	Advanced Normalization Tools
Cingulum-CC	cingulum adjacent to corpus callosum
Cingulum-HC	hippocampal cingulum

### Introduction

Alzheimer's disease (AD) is a progressive neurodegenerative disorder characterized by several hallmark pathologies, including extracellular deposition of beta-amyloid ( $A\beta$ ) plaques (Klunk et al. 2004; Nordberg 2004; Ikonomic et al. 2008), and intracellular aggregation of hyper-phosphorylated tau (Alonso et al. 1996). An important question in AD research is the extent to which these characteristic pathologies – as well as other biomarkers of neural injury – reliably predict neurodegeneration before the onset of dementia. While it is well-known that gray matter (GM) is altered in AD, plaque and tangle pathology are also linked to loss of white matter (WM), comprising myelinated axons (Salat et al. 2009; Balthazar et al. 2009). Furthermore, tau accumulations are pronounced in the axon hillock and are also observed in oligodendroglia (Mietelska-Porowska et al. 2014). Altered microstructure is strongly implicated in the cognitive changes that occur throughout disease progression (Scheltens et al. 1995; Takahashi et al. 2002; Bozzali et al. 2002; Huang et al. 2007; Zhuang et al. 2013). Therefore, elucidating the relationships between biomarkers of AD, and related pathological processing like inflammation, and WM integrity is paramount for understanding both healthy aging and AD. Our mechanistic understanding of aging and AD would also

be improved by a better understanding of which subtypes of neurodegeneration (e.g. axonal, dendritic) affect WM networks during the course of AD development, beginning during the preclinical timeframe.

Diffusion tensor imaging (DTI) is a widely used magnetic resonance technique for assessing brain microstructure *in vivo*, and has enhanced understanding of WM alterations in AD (Stebbins and Murphy 2009; Medina and Gaviria 2008). Among the data that DTI provides, mean diffusivity (MD) and fractional anisotropy (FA) are two of the most commonly studied measures. The important difference between these two metrics is that MD measures the average diffusion across all directions, whereas FA measures diffusion with restricted directionality. As such, MD is sensitive to the average diffusion within a voxel of the brain and can be used as a surrogate marker for cellularity, edema, and necrosis (Alexander et al. 2011). FA is sensitive to diffusion parallel to axons, and changes in FA may reflect loss of myelin or axonal degeneration (Alexander et al. 2011; Bendlin et al. 2010). Several studies have shown that patients with mild cognitive impairment (MCI) or dementia exhibit lower FA and higher MD than controls in brain regions including the temporal lobe WM, the corpus callosum, and the cingulum bundle (Takahashi et al. 2002; Bozzali et al. 2002; Naggara et al. 2006; Medina et al. 2006). Importantly, a multimodal imaging study demonstrated microstructural damage in AD patients independent of gross GM and WM volume loss, suggesting that measurements of WM microstructure provide unique pathophysiological information in regions known to be pivotal in AD (Canu et al. 2011).

In light of several recent studies suggesting that WM alterations contribute to progression from healthy cognition to dementia, it is important to predict and understand the earliest WM changes that may be indicative of future decline in populations that are healthy but at-risk for dementia. Cerebrospinal fluid (CSF) biomarkers have shown value for improving understanding of the evolution of early pathophysiology in AD (Blennow et al. 2010), and may be similarly useful in predicting changes to WM microstructure. It is known that CSF biomarkers are altered before the appearance of clinical symptoms of AD, with levels of  $A\beta$ 42 decreasing in tandem with increasing brain  $A\beta$  plaque deposition (Blennow et al. 2015), and levels of total and phosphorylated tau (p-tau) increasing as the time to diagnosis decreases (Jack et al. 2013; Buchhave et al. 2012). Similarly, markers of axonal and dendritic neurodegeneration, such as neurofilament light protein (NFL) and neurogranin, are predictive of cognitive decline and are elevated in AD patients compared to controls (Henrik Zetterberg et al. 2015; Kvartsberg et al. 2015; Portelius et al. 2015). Finally, markers of inflammation or activated microglia and astrocytes, like chitinase-3-like protein 1 (YKL-40), may serve as proxies for neural injury since inflammation is a response to injured cells and networks

(Olsson et al. 2013). YKL-40 has been shown to be elevated in AD patients compared to controls (Craig-Schapiro et al. 2010; Antonell et al. 2014).

Several studies have used CSF biomarkers in tandem with DTI to assess how biomarkers of pathology predict brain microstructure in incipient or diagnosed dementia due to AD. For instance, a 2011 study found that among 47 individuals with subjective memory complaints or MCI, higher levels of CSF total-tau (t-tau) predicted lower FA in posterior cingulum fibers compared to cognitively healthy control individuals without memory complaints (Stenset et al. 2011). Similarly, another group found that more pathological levels of A $\beta$ 42 and t-tau were associated with reduced FA and increased MD in diffuse WM networks among a larger sample of 78 participants, including those with subjective cognitive complaints, MCI, and AD (Li et al. 2014). Relationships between abnormal CSF biomarkers and altered brain microstructure have also been previously explored in cognitively healthy older adults cross-sectionally. For instance, studies have demonstrated relationships most commonly between DTI measures and CSF A $\beta$ 42, tau, or their ratio (Gold et al. 2014; Molinuevo et al. 2014; Bendlin et al. 2012) but also monocyte chemoattractant protein-1 (Melah et al. 2015). Currently, investigations of longitudinal relationships between CSF biomarkers and brain microstructure are much more limited. It is particularly important to explore this gap in research because WM microstructural patterns may differ depending on the disease stage (Ryan et al. 2013; Kim et al. 2015; Racine et al. 2014) – that is, cross-sectional DTI data may fail to capture the nuances of microstructural change over the course of the AD trajectory, beginning during the preclinical AD stage. In an attempt to understand this time course, Amlien et al. (2013) found that participants with MCI and high levels of CSF t-tau exhibited significant decreases in FA over a two-year time period compared to individuals without MCI or MCI patients without pathological levels of CSF t-tau.

The present study sought to contribute to this research area by investigating the relationship between a more diverse panel of CSF biomarkers and longitudinal changes in brain microstructure in a sample of cognitively healthy older adults at increased risk for AD. In this way, this study aimed to determine the pathological markers most sensitive at predicting alterations in microstructure, including pathology specific to AD (p-tau/A $\beta$ 42), as well as axonal degeneration (NFL), synaptic degeneration (neurogranin), and inflammation (YKL-40) (Mattsson et al. 2016; Henrik Zetterberg and Blennow 2013). We postulated that greater CSF pathology at a baseline time point, and measured longitudinal change over two years, would be indicative of a more rapid progression toward pathological microstructure measured by DTI (e.g. decreasing FA and increasing MD).

## Material and methods

### Participants

Existing data was analyzed in 151 participants from one of two large observational and longitudinally followed cohorts at the University of Wisconsin – Madison. This included people at increased risk for AD due to parental family history (76.16% FH+) in both the Wisconsin Registry for Alzheimer’s Prevention (WRAP;  $n = 127$ , 84.1%) and the Wisconsin Alzheimer’s Disease Research Center (WADRC;  $n = 24$ , 15.9%) if they had undergone at least two DTI scans and at least one lumbar puncture. These cohorts have been described previously (Sager et al. 2005; Kosciak et al. 2014; Racine et al. 2016a; Jonaitis et al. 2013). All participants were cognitively normal at study entry (MCI, AD, and other forms of dementia were excluded). Cohorts did not differ by APOE  $\epsilon$ 4 carriage but did differ on sex and age at baseline MRI; WADRC participants comprised more females compared to WRAP (88% compared to 66%) and were younger on average at their initial MRI ( $56.7 \pm 5.9$  compared to  $61.4 \pm 6.2$ ).

The University of Wisconsin Institutional Review Board approved all study procedures, each participant provided signed informed consent before participation, and all research was completed in accordance with the Helsinki Declaration.

### *DTI acquisition, processing, and signal extraction in regions of interest*

DTI acquisition, image analysis, template creation, and spatial normalization have been described in detail previously (Kim et al. 2015; Racine et al. 2014) and were identical across cohorts. Specifically, all participants were imaged on either one General Electric 3.0 Tesla Discovery MR750 (Waukesha, WI) MRI scanner or a second, identical scanner with 8 channel head coils and parallel imaging (ASSET). DTI was acquired using a diffusion-weighted, spin-echo, single-shot, echo planar imaging (EPI) pulse sequence in 40 encoding directions with  $b = 1300 \text{ s}\cdot\text{mm}^{-2}$ , and eight non-diffusion weighted ( $b = 0$ ) reference images. The cerebrum was covered using contiguous 2.5 mm thick axial slices, FOV = 24 cm, TR = 8000 ms, TE = 67.8 ms, matrix =  $96 \times 96$ , resulting in isotropic  $2.5 \text{ mm}^3$  voxels. High order shimming was performed prior to the DTI acquisition to optimize the homogeneity of the magnetic field across the brain and to minimize EPI distortions. 151 participants had at least two scans, of which  $n = 72$  had a third scan,  $n = 19$  had a fourth scan, and  $n = 3$  had a fifth scan.

While estimating an unbiased atlas (coordinate system) is well investigated in cross-sectional imaging studies, there are fewer validation studies for the longitudinal setting. The additional bias which we must restrict in a longitudinal study is the

interpolation asymmetry that can arise when selecting only one of the time points as a temporal representative in generating the population/study level coordinate system as described in recent works (Yushkevich et al. 2010; Keihaninejad et al. 2013). Based on current best practices, a subject-specific average that is temporally unbiased was first estimated. The subject specific averages were then used to generate an unbiased population level average template space (Fig. 1a). These transformations and the spatial averages are estimated iteratively until convergence. We employed DTI-TK (Zhang et al. 2006, 2007) which is an open source and extensively validated image registration toolbox (Wang et al. 2011; Keihaninejad et al. 2013; Adluru et al. 2012, 2014) for estimating the transformations. Once the unbiased coordinate system was estimated all the scans were registered to this space again using DTI-TK (Fig. 1b).

White matter ROIs were selected a priori due to their previously described sensitivity to changes during MCI and AD, their role in various executive and memory functions, and connectivity to gray matter structures important for memory and executive functions that have been implicated in AD. Specifically, ROIs for the present study (Supplementary Fig. 1) included a global WM mask as well as the left and right cingulum divided into two parts: the cingulum-CC is defined as the portion of the cingulum that runs within the cingulate gyrus, traveling dorsally around the corpus callosum and then transitions to cingulum-HC as it progresses from the splenium of the corpus callosum along the ventral surface of the hippocampus, terminating at entorhinal cortex (Racine et al. 2014). These ROIs were examined in a previous analysis examining the cross-sectional relationship between brain amyloid (measured by PET-PiB imaging) and WM (measured via DTI) acquired at a single time point (Racine et al. 2014). Unlike the previous study, we chose not to examine the fornix because

despite functional interest in this region, CSF partial volume effects in the fornix could make results from DTI difficult to interpret (Baron and Beaulieu 2015), especially in a longitudinal framework. We also added a global WM ROI to capture brain-wide WM metrics.

To obtain the diffusion measures in these ROIs, the JHU-ICBM (Mori et al. 2005) FA template was registered to the unbiased global average (Fig. 1). The individual ROIs were then inverse warped into individual subject space. This is possible because the non-linear transformations estimated using Advanced Normalization Tools (ANTs) are invertible up to numerical accuracy levels. Then to account for any registration imperfections the individual ROIs were thresholded on each diffusion measure map. For FA maps, voxels with FA < 0.2 were excluded because low FA in a region can indicate that the DTI model is not a good fit since there could be crossing fibers or a significant portion of free water signal in that voxel. For all the other measures, first a standard deviation ( $\sigma$ ) of the measure in each ROI is estimated and all the voxels above  $2\sigma$  were excluded to avoid the effect of free water (since free water has largest diffusivities). This step reduces the inclusion of voxels that may show partial volume effects. Risk of partial voluming was also reduced by our registration scheme, which results in near perfect registration across participants of the corpus callosum, which is the structure most likely to be affected by partial voluming from CSF in the lateral ventricles. After these processing refinements of the ROI masks, the mean diffusion measure in each of those ROIs were extracted using `fsstats` and used as outcome measures in our analyses. We chose to examine only FA and MD in these regions because they are the most commonly used metrics and to reduce the number of statistical tests performed. Samples of DTI measurements over time are presented in Supplementary Fig. 2.

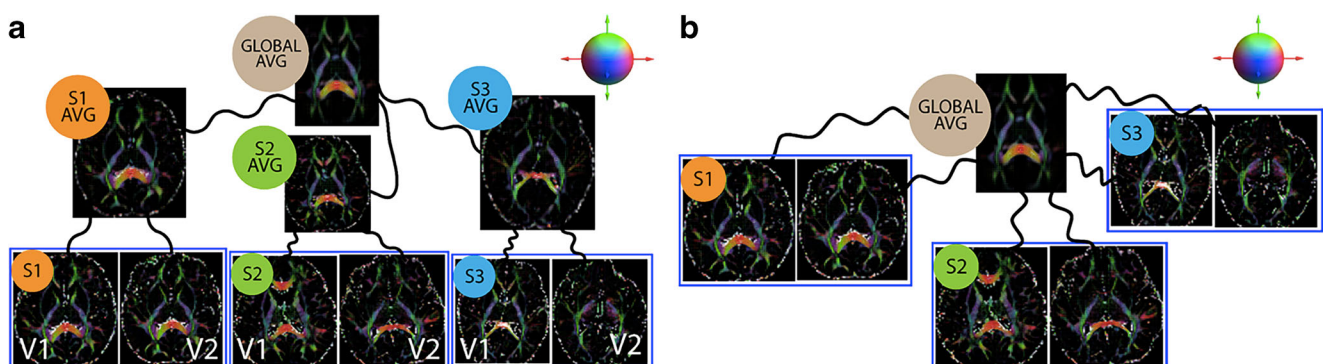


**Fig. 1** Unbiased estimation of the global coordinate system and individual scan registration for the longitudinally acquired imaging data. A) All visit scans were first averaged and then used to estimate the global average. Each image represents the maps of extra-cellular diffusion tensors. B) Individual scans are registered to the unbiased

template. Tensors are color-coded according to their primary orientations as indicated by the color-coded sphere in the top right corners. S1-S3 refers to random subjects each with two imaging visits (V1 and V2). Each of the curved black lines represents a composition of affine and non-linear diffeomorphic transformations

### Cerebrospinal fluid collection and analysis

CSF was collected and assayed as described previously (Starks et al. 2015; E. Portelius et al. 2015; H. Zetterberg et al. 2016) and methods were identical across cohorts. CSF was collected approximately four months after baseline MRI ( $4.34 \pm 12.6$  months). Of the 151 participants with baseline CSF in this study, 91 underwent a second lumbar puncture approximately two years later ( $2.1 \pm 0.40$  years, range 0.69–3.40). Longitudinal CSF data were used to calculate the amount of change in CSF biomarkers ( $\Delta\text{CSF} = \text{CSF level at visit 2} - \text{CSF level at visit 1}$ ) over two years. Positive values for  $\Delta\text{CSF}$  indicate increasing pathology for all CSF biomarkers.

We examined CSF measures for neurodegeneration and inflammation, and a CSF biomarker specific to AD. Respectively, higher levels of NFL, neurogranin, and YKL-40 are indicative of greater axonal degeneration, dendritic degeneration, and astroglial and/or microglial activation and associated inflammation. YKL-40, NFL, and neurogranin were quantified using sandwich enzyme-linked immunosorbent assay (ELISA) (R&D Systems, Minneapolis, Minn., USA; NF-light ELISA kit, Uman Diagnostics AB, Umeå, Sweden; Vmax, Molecular Devices, USA). P-tau/A $\beta$ 42 is a sensitive marker for AD and disease progression (Duits et al. 2014; Fagan et al. 2007; Racine et al. 2016b) which simultaneously captures pathological decreases in CSF A $\beta$ 42 and pathological increases in CSF p-tau, reflecting accumulation of amyloid and neurofibrillary tangle pathology, respectively. P-tau-181 and A $\beta$ 42 were quantified with sandwich ELISAs (INNOTEST Phospho-Tau[181P] and  $\beta$ -amyloid1–42; Fujirebio Europe, Ghent, Belgium).

CSF assays were performed on average 2.1 years apart in two batches. For the entire sample, 116 baseline samples were from batch 1 and 35 were from batch 2. For the analyses in the subset of participants with longitudinal CSF ( $n = 91$ ), all baseline samples were from batch 1 as well as 28 follow-up samples; and 63 follow-up samples were from batch 2. Several studies have indicated that values of a CSF analyte from a single sample can vary from assay batch to batch run due to limitations of the assay technology (Bjerke et al. 2010; Leek et al. 2010). To evaluate batch-to-batch variability and the need for adjusting CSF values for batch in subsequent models, we first conducted a simple linear regression (SLR) analysis for each CSF analyte on a subset of CSF samples that were assayed in both batches ( $n = 96$  from the entire WRAP and WADRC CSF datasets, irrespective of MRI status). Supplementary Fig. 3 depicts the association between the batch 1 and batch 2 samples in this subset analyzed at both batches for the CSF markers under study. SLR was used first to determine whether an analyte differed significantly from batch 1 to 2 (null hypothesis tests of intercept = 0 and slope = 1). If there was insufficient evidence to suggest that either of these hypotheses should be rejected, batch 1 and 2

values were considered comparable. If either of the null hypotheses were rejected, the values used for subsequent analyses for that CSF analyte included batch 1 raw scores when available and batch 1 predicted scores derived from the observed batch 2 raw score and the parameters from the corresponding SLR. All analyses for CSF corrections were performed using R version 3.2.3 using the base “lm” function. Based on these methods, raw values were used for NFL and YKL-40 and predicted values were used for all other CSF variables.

### Statistical analyses

For each CSF variable (baseline or  $\Delta\text{CSF}$ ), DTI metric (FA or MD), and ROI combination we performed a linear mixed effects (LME) model in Stata 13 (StataCorp. 2013. Stata Statistical Software: Release 13. College Station, TX: StataCorp LP) to test our hypotheses that CSF biomarkers of neurodegeneration, inflammation, and AD pathology, or change over time in these biomarkers, would be associated with indicators of worse WM health overall (lower FA and higher MD indicated by model intercepts) and/or progressively worsening WM health over time (decreasing FA and increasing MD indicated by model time-slopes). For each WM ROI and DTI metric, we first conducted unconditional growth models adjusting for random effects of intercept and time-associated slope (at the person level) to determine significant random effects, and then performed conditional models to test our hypotheses. Time was operationalized as interval (years) between MRI visits. Conditional models included significant random effects and fixed effects of the CSF predictor of interest (baseline or  $\Delta\text{CSF}$ ), time, the interaction between CSF predictor and time (baseline CSF  $\times$  time or  $\Delta\text{CSF} \times$  time) as well as covariates of mean-centered age at baseline DTI scan, sex, and cohort. Cohort is a dichotomous variable for study cohort (WADRC or WRAP) included to control for potential latent differences between cohorts. For longitudinal models with  $\Delta\text{CSF}$ , we additionally controlled for lag between the two lumbar punctures, and baseline CSF level to test for effects of CSF change above and beyond those due to baseline CSF level. A significant  $\beta$ -coefficient on a CSF marker or  $\Delta\text{CSF}$  marker indicates that that predictor is associated with the DTI metric overall (main effect), whereas a significant  $\beta$ -coefficient on the CSF predictor  $\times$  time interactions indicate that the CSF predictor is associated with change in the DTI metric over time (increasing/decreasing FA or MD). Thus, we implicitly examined the rate of change in FA and MD by the interactions of CSF  $\times$  time and  $\Delta\text{CSF} \times$  time. Results are evaluated at  $p < .01$ . Trends are reported in supplementary material for  $p < .05$ .

## Results

### Sample characteristics

Sample characteristics are summarized in Table 1.

### Baseline CSF and longitudinal DTI in white matter

Only the biomarkers specific to AD and for inflammation were significantly associated with DTI metrics. P-tau/A $\beta$ 42 was associated with a main effect in MD (higher overall levels) in the left and right cingulum-CC. YKL-40 was associated with a more positive time-slope of MD (increased MD over time) in the left hippocampal cingulum. Significant results ( $p < .01$ ) are displayed in Table 2 and a complete list of results are available in supplementary material (Supplementary Tables 1 and 2). A selection of significant findings are displayed in Fig. 2.

### Change in CSF ( $\Delta$ CSF) and longitudinal DTI in white matter

Only  $\Delta$ neurogranin was significantly associated with FA and MD baseline levels (main effects), but not change in FA or MD over time (slopes). Significant results are displayed in Table 2 and a complete list of results are available in supplementary material (Supplementary Tables 3 and 4). A selection of significant findings are displayed in Fig. 3 (Table 3).

## Discussion

Although protein levels detected from CSF allow indirect measurement of central nervous system pathology, several CSF analytes are associated with relatively distinct aspects of neurodegeneration in the brain. In the present study, we examined CSF markers of AD pathology (p-tau/A $\beta$ 42), axonal degeneration (NFL), dendritic degeneration (neurogranin), and inflammation (YKL-40). By examining both the cross-sectional and longitudinal relationships between these analytes and longitudinally-measured changes in WM microstructure, we sought to better understand the progression of degeneration in select WM networks during late-middle-age and their association with pathology associated with AD. We found that p-tau/A $\beta$ 42 and  $\Delta$ neurogranin were associated with overall levels of FA and MD, and that YKL-40 predicted change in mean diffusivity over time. These results suggest that several CSF biomarkers are correlated with neuroimaging measures of white matter microstructure, but inflammation is the best predictor of progressive white matter degeneration over time.

Previous work by Amlien et al. (2013) that assessed the predictive value of CSF biomarkers on WM integrity showed that high levels of t-tau among MCI patients predicted significant decreases in FA over time. In our study, the only significant association between a CSF biomarker and change in a diffusion metric over time (indicated by a significant interaction of CSF  $\times$  time) was the cingulum-HC mean diffusivity and YKL-40. Additionally, trend-level relationships were noted for p-tau/A $\beta$ 42 and neurogranin (Supplementary Tables 1 and 2). An important difference between our two studies is

**Table 1** Sample characteristics

Sample Characteristics	N	Mean/Frequency	SD	Range
Age at baseline MRI	151	60.3	6.4	44.1 to 79.1
Sex (% female)	151	68.6%		
APOE $\epsilon$ 4 carriage	151	37.3%		
Baseline MRI to LP interval (months)	151	4.34	12.61	–35 to 45
Interval between LPs (months)	91	25.1	4.8	8–40
CSF p-tau/A $\beta$ 42	149	0.061	0.027	0.0236–0.186
CSF Neurogranin	146	387.29	177.97	125.00–957.84
CSF YKL-40	151	145,033.88	51,388.87	49,994.00–335,820.87
CSF NFL	150	625.25	243.15	222.00–2030.00
$\Delta$ CSF p-tau/A $\beta$ 42	89	0.007	0.016	–0.037 – 0.060
$\Delta$ CSF Neurogranin	86	32.75	118.84	–417.93 – 657.13
$\Delta$ CSF YKL-40	91	11,025.99	21,155.65	–41,812.00 – 99,199.11
$\Delta$ CSF NFL	89	80.510	207.76	–984.00 – 1070.00

All CSF values are in ng/L. N's varied due to assay sensitivity/variability

APOE apolipoprotein, MRI Magnetic Resonance Imaging, LP lumbar puncture, CSF cerebrospinal fluid, p-tau/A $\beta$ 42 phosphorylated-tau to beta-amyloid-42 ratio, YKL-40 chitinase-3-like protein, NFL neurofilament light protein, SD standard deviation

**Table 2** Significant associations between baseline CSF levels and mean diffusivity

CSF Biomarker (model parameter)	White Matter ROI	$\beta$	Standard Error	Z-statistic	95% Confidence Interval	P-value
P-tau/A $\beta$ 42 (main effect)	Right Cingulum-CC	0.247	0.087	2.83	0.076, 0.418	0.005
P-tau/A $\beta$ 42 (main effect)	Left Cingulum-CC	0.282	0.103	2.74	0.080, 0.485	0.006
YKL-40 $\times$ time (slope)	Left Cingulum-HC	0.000310	0.000087	3.13	0.000116, 0.000504	0.002

CSF cerebrospinal fluid, ROI region of interest, p-tau/A $\beta$ 42 phosphorylated-tau to beta-amyloid-42 ratio, YKL-40 chitinase-3-like protein, CC corpus callosum, HC hippocampus

that our measurements occurred during late middle age and possibly the presymptomatic phase of AD, rather than a clinically symptomatic phase like MCI. It is possible that different

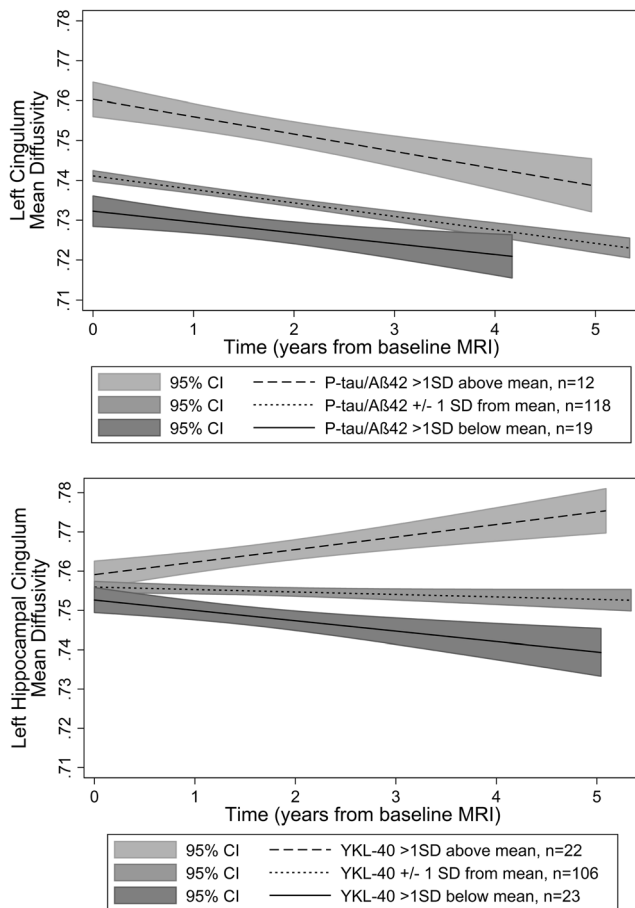


**Fig. 2** Predicted associations between baseline CSF biomarker levels of p-tau/A $\beta$ 42 and YKL-40 and longitudinally-measured white matter mean diffusivity. Top panel: higher p-tau/A $\beta$ 42 levels were associated with higher MD at baseline (intercept) but not change over time (slopes are not significantly different from zero) in the cingulum bundle adjacent to the corpus callosum. Bottom panel: higher YKL-40 levels were associated with increasing MD over time (slope) but were not associated with baseline MD (intercept). Although the CSF variables were analyzed as continuous predictors, for visualization purposes they are displayed as high (CSF levels >1 SD above the mean, dashed line), mean (CSF levels within 1 SD of the mean, dotted line), and low (CSF levels >1 SD below the mean, solid line). Y-axis: Mean Diffusivity (MD) in the specified ROI. X-axis: Time operationalized as interval from baseline MRI in years. 95% Confidence Intervals (C.I.'s) are displayed by the gray shaded regions

underlying mechanisms may drive white matter degeneration during different phases of AD, highlighting the importance of continued research on longitudinal changes in brain health, beginning during middle age and continuing into symptomatic phases of the disease.

Slight differences in findings between the neural injury markers suggest that certain types of neural injury differentially affect WM tracts, and the fact that YKL-40 was a particularly robust predictor for WM deterioration is in line with recent research implicating inflammation in the progression to dementia. Not only has it been shown that YKL-40 is generally higher among AD patients than age-matched healthy controls (Rosén et al. 2014; Wildsmith et al. 2014), but inflammation may be a particularly important phenomenon early in AD progression. This is evidenced by a significant difference in YKL-40 plasma and CSF concentrations in patients with early AD compared to healthy controls, but no difference in late stage AD patients compared to healthy controls (Choi et al. 2011; Antonell et al. 2014). Perhaps more compellingly, biomarkers of inflammation have also proved to be useful predictors of microstructural pathology even in a group of asymptomatic late-middle-aged adults, whereby YKL-40 was associated with higher NFL and total tau in the CSF (Melah et al. 2015).

Although the sample size was smaller, the analyses examining longitudinal change in CSF markers provided additional insights into the evolving relationship between AD-related pathology and WM pathology. We found that increases in  $\Delta$ neurogranin were associated with lower FA and higher MD. Neurogranin is a post-synaptic neuronal protein that is thought to be involved in synaptic plasticity, synaptic regeneration, long-term potentiation, and learning and memory (Pak et al. 2000; Diez-Guerra 2010; Blennow and Zetterberg 2015). Levels of neurogranin have been shown to be elevated in AD, predict conversion from MCI to AD, and predict cognitive decline in cognitively normal individuals (Tarawneh et al. 2016; Kester et al. 2015). Here we show that elevated neurogranin levels are also associated with a possible biological substrate of that decline, impaired WM integrity.

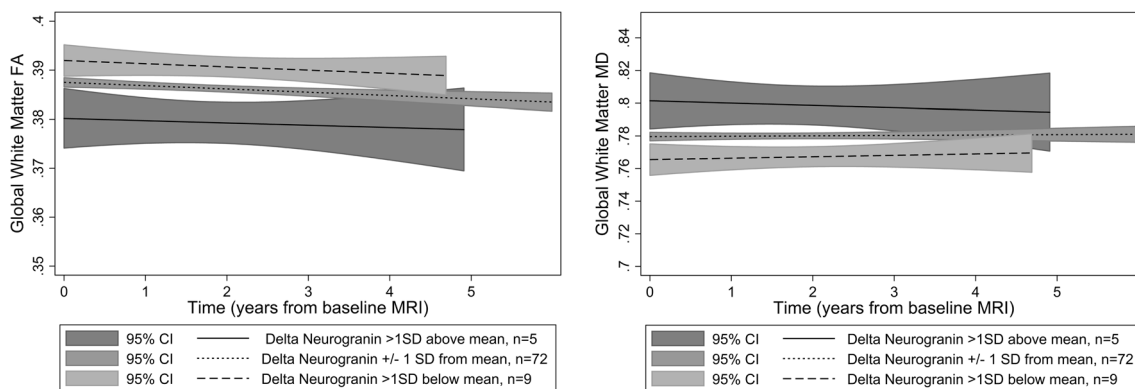


**Fig. 3** Predicted associations between  $\Delta$ CSF biomarkers levels of neurogranin and longitudinally-measured white matter diffusion metrics in global white matter. Larger increases in neurogranin ( $\Delta$ neurogranin) were associated with lower FA (left) and higher MD (right) overall, but not with change over time (slopes are not significantly different from zero). Although  $\Delta$ CSF variables were analyzed as continuous predictors, for visualization purposes they are displayed as high ( $\Delta$  values greater

than 1 SD above the mean, solid line), mean ( $\Delta$  values within 1 SD of the mean, dotted line), and low ( $\Delta$  values  $>1$  SD below the mean, dashed line). Y-axis: Fractional Anisotropy (FA, left) or Mean Diffusivity (MD, right) in the global white matter region of interest. X-axis: Time operationalized as interval from baseline MRI in years. 95% Confidence Intervals (C.I.'s) are displayed by the gray shaded regions

Unlike other studies, we did not find that compared to baseline levels that change in CSF biomarkers greatly enhanced the prediction of white matter changes. In contrast, in a retrospective analysis, Stomrud et al. (2010) found that change (but not baseline) CSF levels of  $A\beta_{42}$  and p-tau predicted subsequent cognitive decline in a healthy older adult cohort. Additionally, Sutphen et al. (2015) found that increasing levels of t-tau, p-tau, YKL-40, and VILIP-1 (a marker of neuronal death) were associated with brain amyloid positivity measured by PET-PiB. They further found that the majority of participants who progressed from a CDR of 0 to a CDR of 0.5 or 1 exhibited low  $A\beta_{42}$  and  $A\beta_{42}/A\beta_{40}$  at baseline and follow-up as well as high total tau and t-tau/ $A\beta_{42}$ . Because we found that at a trend level (Supplementary Table 4)  $\Delta$ p-tau/ $A\beta_{42}$  was associated with increasing mean diffusivity in the left cingulum-CC, it is likely that the smaller sample size for our longitudinal analyses restricted our power to detect some relationships. An additional consideration is the interval between the lumbar punctures. A necessary interval to detect meaningful change—as well as how to define meaningful change—during different stages of AD remains an important area for further study.

It should be noted that our interpretations are further limited by the fact that both CSF and DTI are indirect measures of

biological processes and that our longitudinal measurements of both biomarkers are restricted to a relatively short interval when considered in the context of aging and age-related diseases, which unfold over decades. Development of universal cut-points for CSF biomarker positivity will be an important step in advancing our understanding of the clinical applications of the present work, and could facilitate investigations of interactions among different measures of AD-related pathology. Additionally, given that MD and FA can be influenced by changes in radial and axial diffusivity, future studies should expand upon this work by determining to what extent the present findings can be explained by changes in these metrics. This may provide more insight into the biological underpinnings of the DTI measures examined here. Similarly, future studies may consider using exploratory methods like tract-based spatial statistics in a longitudinal framework to investigate additional white matter regions that were not analyzed in this hypothesis-driven study. Although hypothesis-driven ROI approaches are always accompanied with risk of missing important associations in regions of the brain not examined, we chose to perform an ROI-based analysis rather than a voxel-wise approach across the entire brain because (1) we had a priori hypotheses based on prior work from our group and others about where the strongest associations were

**Table 3** Significant associations between baseline CSF levels and diffusion metrics

CSF biomarker (model parameter)	WM ROI (DTI metric)	$\beta$	Standard Error	Z-statistic	95% Confidence Interval	P-value
$\Delta$ Neurogranin (main effect)	Global WM Mask (FA)	−.0000261	.0000101	−2.59	−.0000458, −6.36e-06	0.01
$\Delta$ Neurogranin (main effect)	Global WM Mask (MD)	0.000771	0.000194	3.97	0.000391, 0.00115	< 0.001
$\Delta$ Neurogranin (main effect)	Right Cingulum-CC (MD)	0.000112	0.000259	4.31	0.000061, 0.00166	< 0.001
$\Delta$ Neurogranin (main effect)	Left Cingulum-CC (MD)	0.00111	0.000332	3.34	0.000458, 0.00176	0.001

CSF cerebrospinal fluid, ROI region of interest, CC corpus callosum, WM white matter, MD mean diffusivity, FA fractional anisotropy

expected to occur, (2) the statistical signal in the case of pre-clinical AD is known to be small, and we wanted to reduce risk of Type II errors that are likely to occur with the substantial correction for multiple comparisons required in voxel-wise analyses, and (3) methods for improving sensitivity to DTI change over time are under development; this will be a critical area for future research as these emergent techniques evolve.

Despite these limitations, this study provides important insights into the evolving relationship between CSF markers of neural injury and WM microstructure in an aging middle-aged cohort enriched with risk for AD due to parental family history. We found that markers of CSF (i.e., baseline values or change values) were associated with DTI metrics and that the rate of time-related change in DTI was increased by some CSF biomarker levels. Our results support the hypothesis that CSF indicators of AD-related pathology are associated with DTI metrics of impaired WM health. An important next step will be to replicate these findings under different methodologies. For instance, voxel-wise linear mixed effects modeling is an emerging technique that allows for assessment of brain changes over time and has recently been used to examine differences between healthy controls, MCI, and AD patients (Chen et al. 2013; Bernal-Rusiel et al. 2013). Additionally, multi-resolution graph wavelet techniques, which have been shown to increase statistical sensitivity and improve statistical power to examine global brain changes with correction for multiple comparisons, could extend the present work by investigating subtle but important relationships between white matter and CSF across the entire brain (Kim et al. 2012, 2013, 2014). Future studies are planned to employ these innovative technologies to the present cohort. Another critical follow-up will be to connect these longitudinal biomarker changes to cognitive decline and diagnosed disease. Additionally, while significant change in CSF biomarkers may occur over two years, greater and more clinically meaningful change may be detected using more frequent data collection and longer intervals. Studies of these participants are ongoing, and the results from the current study will be especially useful in the context of future longitudinal assessments.

**Acknowledgements** The authors gratefully acknowledge Amy Hawley, Jennifer Oh, Chuck Illingworth, Nancy Davenport-Sis, Sandra Harding, and the support of researchers and staff at the Wisconsin Alzheimer's Disease Research Center, the Wisconsin Alzheimer's Institute, the Waisman Center, and the University of Wisconsin-Madison for their assistance in recruitment, data collection, and data analysis. Above all, we wish to thank our dedicated volunteers for their participation in this research.

#### Compliance with ethical standards

**Funding** This research was supported by the National Institutes of Health awards (AG021155, AG027161, AG000213, P50 AG033514, AG037639 and UL1RR025011) to the University of Wisconsin,

Madison; by the National Science Foundation Graduate Research Fellowship under Grant No. DGE-1256259 (APM); by the Neuroscience & Public Policy Program (SES-0849122); by the Neuroscience Training Program (T32GM007507); by the Medical Scientist Training Program (T32GM008692); by the Wisconsin Alzheimer's Institute Lou Holland Fund; and by the Swedish Research Council, the Swedish Brain Foundation, the Knut and Alice Wallenberg Foundation, and Torsten Söderberg's Foundation to the University of Gothenburg. N.A is supported in part by R01-EB022883, U54-HD090256, U54-AI117924, UF1-AG051216 and R56-AG052698. The project was also supported by the Clinical and Translational Science Award (CTSA) program by the National Center for Advancing Translational Sciences (NCATS) grant UL1TR000427 and NSF CAREER award (1252725). Portions of this research were supported by the Veterans Administration including facilities and resources at the Geriatric Research Education and Clinical Center of the William S. Middleton Memorial Veterans Hospital, Madison, WI. Any opinions, findings, and conclusions or recommendations expressed in this material are those of the authors(s) and do not necessarily reflect the views of the NIH, the Veterans Administration, or National Science Foundation.

**Conflict of interest** KB and HZ are co-founders of Brain Biomarker Solutions in Gothenburg AB, a GU Venture-based platform company at the University of Gothenburg. KB has served as a consultant or at advisory boards for IBL International, Roche Diagnostics, Eli Lilly, Fujirebio Europe, and Novartis. The other authors declare that they have no conflict of interest.

**Ethical approval** All procedures performed in studies involving human participants were in accordance with the ethical standards of the institutional and/or national research committee and with the 1964 Helsinki declaration and its later amendments or comparable ethical standards.

**Informed consent** Informed consent was obtained from all individual participants included in the study.

## References

- Adluru, N., Zhang, H., Fox, A. S., Shelton, S. E., Ennis, C. M., Bartosic, A. M., et al. (2012). A diffusion tensor brain template for rhesus macaques. *NeuroImage*, *59*(1), 306–318.
- Adluru, N., Destiche, D. J., Lu, S. Y.-F., Doran, S. T., Birdsill, A. C., Melah, K. E., et al. (2014). White matter microstructure in late middle-age: Effects of apolipoprotein E4 and parental family history of Alzheimer's disease. *NeuroImage: Clinical*, *4*, 730–742.
- Alexander, A. L., Hurley, S. A., Samsonov, A. A., Adluru, N., Hosseinbor, A. P., Mossahebi, P., et al. (2011). Characterization of cerebral white matter properties using quantitative magnetic resonance imaging stains. *Brain Connectivity*, *1*(6), 423–446.
- Alonso, A. d. C., Grundke-Iqbal, I., & Iqbal, K. (1996). Alzheimer's disease hyperphosphorylated tau sequesters normal tau into tangles of filaments and disassembles microtubules. *Nature Medicine*, *2*(7), 783–787.
- Amlien, I. K., Fjell, A. M., Walhovd, K. B., Selnes, P., Stenset, V., Grambaite, R., et al. (2013). Mild cognitive impairment: Cerebrospinal fluid tau biomarker pathologic levels and longitudinal changes in white matter integrity. *Radiology*, *266*(1), 295–303.
- Antonell, A., Mansilla, A., Rami, L., Lladó, A., Iranzo, A., Olives, J., et al. (2014). Cerebrospinal fluid level of YKL-40 protein in preclinical and prodromal Alzheimer's disease. *Journal of Alzheimer's Disease*, *42*(3), 901–908.

- Balthazar, M., Yasuda, C., Pereira, F., Pedro, T., Damasceno, B., & Cendes, F. (2009). Differences in grey and white matter atrophy in amnesic mild cognitive impairment and mild Alzheimer's disease. *European Journal of Neurology*, *16*(4), 468–474.
- Baron, C. A., & Beaulieu, C. (2015). Acquisition strategy to reduce cerebrospinal fluid partial volume effects for improved DTI tractography. *Magnetic Resonance in Medicine*, *73*(3), 1075–1084. doi:10.1002/mrm.25226.
- Bendlin, B. B., Fitzgerald, M. E., Ries, M. L., Xu, G., Kastman, E. K., Thiel, B. W., et al. (2010). White matter in aging and cognition: A cross-sectional study of microstructure in adults aged eighteen to eighty-three. *Developmental Neuropsychology*, *35*(3), 257–277.
- Bendlin, B. B., Carlsson, C. M., Johnson, S. C., Zetterberg, H., Blennow, K., Willette, A. A., et al. (2012). CSF T-tau/A $\beta$  42 predicts white matter microstructure in healthy adults at risk for Alzheimer's disease. *PLoS One*, *7*(6), e37720.
- Bernal-Rusiel, J. L., Reuter, M., Greve, D. N., Fischl, B., Sabuncu, M. R., & Initiative, A. S. D. N. (2013). Spatiotemporal linear mixed effects modeling for the mass-univariate analysis of longitudinal neuroimage data. *NeuroImage*, *81*, 358–370.
- Bjerke, M., Portelius, E., Minthon, L., Wallin, A., Anckarsäter, H., Anckarsäter, R., et al. (2010). Confounding factors influencing amyloid beta concentration in cerebrospinal fluid. *International journal of Alzheimer's disease*, 2010. doi:10.4061/2010/986310.
- Blennow, K., & Zetterberg, H. (2015). The past and the future of Alzheimer's disease CSF biomarkers—A journey toward validated biochemical tests covering the whole spectrum of molecular events. *Frontiers in Neuroscience*, *9* (2015): 345. doi:10.3389/fnins.2015.00345.
- Blennow, K., Hampel, H., Weiner, M., & Zetterberg, H. (2010). Cerebrospinal fluid and plasma biomarkers in Alzheimer disease. *Nature Reviews Neurology*, *6*(3), 131–144.
- Blennow, K., Dubois, B., Fagan, A. M., Lewczuk, P., de Leon, M. J., & Hampel, H. (2015). Clinical utility of cerebrospinal fluid biomarkers in the diagnosis of early Alzheimer's disease. *Alzheimer's & Dementia*, *11*(1), 58–69.
- Bozzali, M., Falini, A., Franceschi, M., Cercignani, M., Zuffi, M., Scotti, G., et al. (2002). White matter damage in Alzheimer's disease assessed in vivo using diffusion tensor magnetic resonance imaging. *Journal of Neurology, Neurosurgery & Psychiatry*, *72*(6), 742–746.
- Buchhave, P., Minthon, L., Zetterberg, H., Wallin, Å. K., Blennow, K., & Hansson, O. (2012). Cerebrospinal fluid levels of  $\beta$ -amyloid 1–42, but not of tau, are fully changed already 5 to 10 years before the onset of Alzheimer dementia. *Archives of General Psychiatry*, *69*(1), 98–106.
- Canu, E., McLaren, D. G., Fitzgerald, M. E., Bendlin, B. B., Zoccatelli, G., Alessandrini, F., et al. (2011). Mapping the structural brain changes in Alzheimer's disease: The independent contribution of two imaging modalities. *Journal of Alzheimer's Disease*, *26*(s3), 263–274.
- Chen, G., Saad, Z. S., Britton, J. C., Pine, D. S., & Cox, R. W. (2013). Linear mixed-effects modeling approach to fMRI group analysis. *NeuroImage*, *73*, 176–190.
- Choi, J., Lee, H.-W., & Suk, K. (2011). Plasma level of chitinase 3-like 1 protein increases in patients with early Alzheimer's disease. *Journal of Neurology*, *258*(12), 2181–2185.
- Craig-Schapiro, R., Perrin, R. J., Roe, C. M., Xiong, C., Carter, D., Cairns, N. J., et al. (2010). YKL-40: A novel prognostic fluid biomarker for preclinical Alzheimer's disease. *Biological Psychiatry*, *68*(10), 903–912.
- Diez-Guerra, F. J. (2010). Neurogranin, a link between calcium/calmodulin and protein kinase C signaling in synaptic plasticity. *IUBMB Life*, *62*(8), 597–606. doi:10.1002/iub.357.
- Duits, F. H., Teunissen, C. E., Bouwman, F. H., Visser, P.-J., Mattsson, N., Zetterberg, H., et al. (2014). The cerebrospinal fluid “Alzheimer profile”: Easily said, but what does it mean? *Alzheimer's & Dementia*, *10*(6), 713–723. e712.
- Fagan, A. M., Roe, C. M., Xiong, C., Mintun, M. A., Morris, J. C., & Holtzman, D. M. (2007). Cerebrospinal fluid tau/ $\beta$ -amyloid42 ratio as a prediction of cognitive decline in nondemented older adults. *Archives of Neurology*, *64*(3), 343–349.
- Gold, B. T., Zhu, Z., Brown, C. A., Andersen, A. H., LaDu, M. J., Tai, L., et al. (2014). White matter integrity is associated with cerebrospinal fluid markers of Alzheimer's disease in normal adults. *Neurobiology of Aging*, *35*(10), 2263–2271.
- Huang, J., Friedland, R., & Auchus, A. (2007). Diffusion tensor imaging of normal-appearing white matter in mild cognitive impairment and early Alzheimer disease: Preliminary evidence of axonal degeneration in the temporal lobe. *American Journal of Neuroradiology*, *28*(10), 1943–1948.
- Ikonomic, M. D., Klunk, W. E., Abrahamson, E. E., Mathis, C. A., Price, J. C., Tsopelas, N. D., et al. (2008). Post-mortem correlates of in vivo PiB-PET amyloid imaging in a typical case of Alzheimer's disease. *Brain*, *131*(6), 1630–1645.
- Jack, C. R., Knopman, D. S., Jagust, W. J., Petersen, R. C., Weiner, M. W., Aisen, P. S., et al. (2013). Tracking pathophysiological processes in Alzheimer's disease: An updated hypothetical model of dynamic biomarkers. *The Lancet Neurology*, *12*(2), 207–216. doi:10.1016/S1474-4422(12)70291-0.
- Jonaitis, E., La Rue, A., Mueller, K. D., Kosciak, R. L., Hermann, B., & Sager, M. A. (2013). Cognitive activities and cognitive performance in middle-aged adults at risk for Alzheimer's disease. *Psychology and Aging*, *28*(4), 1004.
- Keihaninejad, S., Zhang, H., Ryan, N. S., Malone, I. B., Modat, M., Cardoso, M. J., et al. (2013). An unbiased longitudinal analysis framework for tracking white matter changes using diffusion tensor imaging with application to Alzheimer's disease. *NeuroImage*, *72*, 153–163.
- Kester, M. I., Teunissen, C. E., Crimmins, D. L., Herries, E. M., Ladenson, J. H., Scheltens, P., et al. (2015). Neurogranin as a cerebrospinal fluid biomarker for synaptic loss in symptomatic Alzheimer disease. *JAMA Neurology*, *72*(11), 1275–1280. doi:10.1001/jamaneurol.2015.1867.
- Kim, W. H., Pachauri, D., Hatt, C., Chung, M. K., Johnson, S. C., & Singh, V. (2012). Wavelet based multi-scale shape features on arbitrary surfaces for cortical thickness discrimination. *Advance in Neural Information Processing Systems*, 2012, 1241–1249.
- Kim, W. H., Adluru, N., Chung, M. K., Charchut, S., GadElkarim, J. J., Altshuler, L., et al. (2013). Multi-resolutional brain network filtering and analysis via wavelets on non-Euclidean space. Medical image computing and computer-assisted intervention : MICCAI ... International Conference on Medical Image Computing and Computer-Assisted Intervention, 16(Pt 3), 643–651.
- Kim, W. H., Singh, V., Chung, M. K., Hinrichs, C., Pachauri, D., Okonkwo, O. C., et al. (2014). Multi-resolutional shape features via non-Euclidean wavelets: Applications to statistical analysis of cortical thickness. *NeuroImage*, *93*(Pt 1), 107–123. doi:10.1016/j.neuroimage.2014.02.028.
- Kim, W. H., Adluru, N., Chung, M. K., Okonkwo, O. C., Johnson, S. C., Bendlin, B. B., et al. (2015). Multi-resolution statistical analysis of brain connectivity graphs in preclinical Alzheimer's disease. *NeuroImage*, *118*, 103–117. doi:10.1016/j.neuroimage.2015.05.050.
- Klunk, W. E., Engler, H., Nordberg, A., Wang, Y., Blomqvist, G., Holt, D. P., et al. (2004). Imaging brain amyloid in Alzheimer's disease with Pittsburgh compound-B. *Annals of Neurology*, *55*(3), 306–319.
- Kosciak, R. L., La Rue, A., Jonaitis, E. M., Okonkwo, O. C., Johnson, S. C., Bendlin, B. B., et al. (2014). Emergence of mild cognitive impairment in late middle-aged adults in the Wisconsin Registry for Alzheimer's Prevention. *Dementia and Geriatric Cognitive Disorders*, *38*(1–2), 16–30.

- Kvartberg, H., Duits, F. H., Ingelsson, M., Andreasen, N., Öhrfelt, A., Andersson, K., et al. (2015). Cerebrospinal fluid levels of the synaptic protein neurogranin correlates with cognitive decline in prodromal Alzheimer's disease. *Alzheimer's & Dementia*, *11*(10), 1180–1190.
- Leek, J. T., Scharpf, R. B., Bravo, H. C., Simcha, D., Langmead, B., Johnson, W. E., et al. (2010). Tackling the widespread and critical impact of batch effects in high-throughput data. *Nature Reviews Genetics*, *11*(10), 733–739. doi:10.1038/nrg2825.
- Li, X., Li, T. Q., Andreasen, N., Wiberg, M., Westman, E., & Wahlund, L. O. (2014). The association between biomarkers in cerebrospinal fluid and structural changes in the brain in patients with Alzheimer's disease. *Journal of Internal Medicine*, *275*(4), 418–427.
- Mattsson, N., Insel, P. S., Palmqvist, S., Portelius, E., Zetterberg, H., Weiner, M., et al. (2016). Cerebrospinal fluid tau, neurogranin, and neurofilament light in Alzheimer's disease. *EMBO Molecular Medicine*, *8*(10), 1184–1196.
- Medina, D. A., & Gaviria, M. (2008). Diffusion tensor imaging investigations in Alzheimer's disease: The resurgence of white matter compromise in the cortical dysfunction of the aging brain. *Neuropsychiatric Disease and Treatment*, *4*(4), 737–742.
- Medina, D. A., Urresta, F., Gabrieli, J. D., Moseley, M., Fleischman, D., Bennett, D. A., et al. (2006). White matter changes in mild cognitive impairment and AD: A diffusion tensor imaging study. *Neurobiology of Aging*, *27*(5), 663–672.
- Melah, K. E., Lu, S. Y., Hoscheidt, S. M., Alexander, A. L., Adluru, N., Destiche, D. J., et al. (2015). Cerebrospinal fluid markers of Alzheimer's disease pathology and microglial activation are associated with altered white matter microstructure in asymptomatic adults at risk for Alzheimer's disease. *Journal of Alzheimer's disease : JAD*, *50*(3), 873–886. doi:10.3233/JAD-150897.
- Mietelska-Porowska, A., Wasik, U., Goras, M., Filipek, A., & Niewiadomska, G. (2014). Tau protein modifications and interactions: Their role in function and dysfunction. *International Journal of Molecular Sciences*, *15*(3), 4671–4713. doi:10.3390/ijms15034671.
- Molinieuo, J. L., Ripolles, P., Simó, M., Lladó, A., Olives, J., Balasa, M., et al. (2014). White matter changes in preclinical Alzheimer's disease: A magnetic resonance imaging-diffusion tensor imaging study on cognitively normal older people with positive amyloid  $\beta$  protein 42 levels. *Neurobiology of Aging*, *35*(12), 2671–2680.
- Mori, S., Wakana, S., Van Zijl, P. C., & Nagae-Poetscher, L. (2005). *MRI atlas of human white matter* (Vol. 16): Am Soc neuroradiology.
- Naggara, O., Oppenheim, C., Rieu, D., Raoux, N., Rodrigo, S., Dalla Barba, G., et al. (2006). Diffusion tensor imaging in early Alzheimer's disease. *Psychiatry Research: Neuroimaging*, *146*(3), 243–249.
- Nordberg, A. (2004). PET imaging of amyloid in Alzheimer's disease. *The Lancet Neurology*, *3*(9), 519–527.
- Olsson, B., Hertze, J., Lautner, R., Zetterberg, H., Nagga, K., Hoglund, K., et al. (2013). Microglial markers are elevated in the prodromal phase of Alzheimer's disease and vascular dementia. *Journal of Alzheimer's disease: JAD*, *33*(1), 45–53. doi:10.3233/JAD-2012-120787.
- Pak, J. H., Huang, F. L., Li, J., Balschun, D., Reymann, K. G., Chiang, C., et al. (2000). Involvement of neurogranin in the modulation of calcium/calmodulin-dependent protein kinase II, synaptic plasticity, and spatial learning: A study with knockout mice. *Proceedings of the National Academy of Sciences of the United States of America*, *97*(21), 11232–11237. doi:10.1073/pnas.210184697.
- Portelius, E., Zetterberg, H., Skillbäck, T., Törnqvist, U., Andreasson, U., Trojanowski, J. Q., et al. (2015). Cerebrospinal fluid neurogranin: Relation to cognition and neurodegeneration in Alzheimer's disease. *Brain*, *138*(11), 3373–3385. doi:10.1093/brain/awv267.
- Racine, A. M., Adluru, N., Alexander, A. L., Christian, B. T., Okonkwo, O. C., Oh, J., et al. (2014). Associations between white matter microstructure and amyloid burden in preclinical Alzheimer's disease: A multimodal imaging investigation. *NeuroImage: Clinical*, *4*, 604–614.
- Racine, A. M., Kosciak, R. L., Berman, S. E., Nicholas, C. R., Clark, L. R., Okonkwo, O. C., et al. (2016a). Biomarker clusters are differentially associated with longitudinal cognitive decline in late midlife. *Brain*, *139*(8), 2261–2274. doi:10.1093/brain/aww142.
- Racine, A. M., Kosciak, R. L., Nicholas, C. R., Clark, L. R., Okonkwo, O. C., Oh, J. M., et al. (2016b). Cerebrospinal fluid ratios with A $\beta$  42 predict preclinical brain  $\beta$ -amyloid accumulation. *Alzheimer's & Dementia: Diagnosis, Assessment & Disease Monitoring*, *2*, 27–38.
- Rosén, C., Andersson, C.-H., Andreasson, U., Molinuevo, J. L., Bjerke, M., Rami, L., et al. (2014). Increased levels of chitotriosidase and YKL-40 in cerebrospinal fluid from patients with Alzheimer's disease. *Dementia and Geriatric Cognitive Disorders Extra*, *4*(2), 297–304.
- Ryan, N. S., Keihaninejad, S., Shakespeare, T. J., Lehmann, M., Crutch, S. J., Malone, I. B., et al. (2013). Magnetic resonance imaging evidence for presymptomatic change in thalamus and caudate in familial Alzheimer's disease. *Brain*, *136*(5), 1399–1414.
- Sager, M. A., Hermann, B., & La Rue, A. (2005). Middle-aged children of persons with Alzheimer's disease: APOE genotypes and cognitive function in the Wisconsin Registry for Alzheimer's Prevention. *Journal of Geriatric Psychiatry and Neurology*, *18*(4), 245–249.
- Salat, D. H., Greve, D. N., Pacheco, J. L., Quinn, B. T., Helmer, K. G., Buckner, R. L., et al. (2009). Regional white matter volume differences in nondemented aging and Alzheimer's disease. *NeuroImage*, *44*(4), 1247–1258. doi:10.1016/j.neuroimage.2008.10.030.
- Scheltens, P., Barkhof, F., Leys, D., Wolters, E. C., Ravid, R., & Kamphorst, W. (1995). Histopathologic correlates of white matter changes on MRI in Alzheimer's disease and normal aging. *Neurology*, *45*(5), 883–888.
- Starks, E. J., Patrick O'Grady, J., Hoscheidt, S. M., Racine, A. M., Carlsson, C. M., Zetterberg, H., et al. (2015). Insulin resistance is associated with higher cerebrospinal fluid tau levels in asymptomatic APOE $\epsilon$ 4 carriers. *Journal of Alzheimer's Disease*, *46*(2), 525–533.
- Stebbins, G. T., & Murphy, C. M. (2009). Diffusion tensor imaging in Alzheimer's disease and mild cognitive impairment. *Behavioural Neurology*, *21*(1), 39–49. doi:10.3233/BEN-2009-0234.
- Stenset, V., Bjørnerud, A., Fjell, A. M., Walhovd, K. B., Hofoss, D., Due-Tønnessen, P., et al. (2011). Cingulum fiber diffusivity and CSF T-tau in patients with subjective and mild cognitive impairment. *Neurobiology of Aging*, *32*(4), 581–589.
- Stomrud, E., Hansson, O., Zetterberg, H., Blennow, K., Minthon, L., & Londos, E. (2010). Correlation of longitudinal cerebrospinal fluid biomarkers with cognitive decline in healthy older adults. *Archives of Neurology*, *67*(2), 217–223.
- Suthphen, C. L., Jasielc, M. S., Shah, A. R., Macy, E. M., Xiong, C., Vlassenko, A. G., et al. (2015). Longitudinal cerebrospinal fluid biomarker changes in preclinical Alzheimer disease during middle age. *JAMA Neurology*. doi:10.1001/jamaneurol.2015.1285.
- Takahashi, S., Yonezawa, H., Takahashi, J., Kudo, M., Inoue, T., & Tohgi, H. (2002). Selective reduction of diffusion anisotropy in white matter of Alzheimer disease brains measured by 3.0 tesla magnetic resonance imaging. *Neuroscience Letters*, *332*(1), 45–48.
- Tarawneh, R., D'Angelo, G., Crimmins, D., Herries, E., Griest, T., Fagan, A. M., et al. (2016). Diagnostic and prognostic utility of the synaptic marker Neurogranin in Alzheimer disease. *JAMA Neurology*, *73*(5), 561–571. doi:10.1001/jamaneurol.2016.0086.
- Wang, Y., Gupta, A., Liu, Z., Zhang, H., Escobar, M. L., Gilmore, J. H., et al. (2011). DTI registration in atlas based fiber analysis of infantile Krabbe disease. *NeuroImage*, *55*(4), 1577–1586.
- Wildsmith, K. R., Schauer, S. P., Smith, A. M., Arnott, D., Zhu, Y., Haznedar, J., et al. (2014). Identification of longitudinally dynamic biomarkers in Alzheimer's disease cerebrospinal fluid by targeted proteomics. *Molecular Neurodegeneration*, *9*, 22.

- Yushkevich, P. A., Avants, B. B., Das, S. R., Pluta, J., Altinay, M., Craige, C., et al. (2010). Bias in estimation of hippocampal atrophy using deformation-based morphometry arises from asymmetric global normalization: An illustration in ADNI 3 T MRI data. *NeuroImage*, *50*(2), 434–445.
- Zetterberg, H., & Blennow, K. (2013). Cerebrospinal fluid biomarkers for Alzheimer's disease: More to come? *Journal of Alzheimer's Disease*, *33*(s1), S361–S369.
- Zetterberg, H., Skillbäck, T., Mattsson, N., Trojanowski, J. Q., Portelius, E., Shaw, L. M., et al. (2015). Association of Cerebrospinal Fluid Neurofilament Light Concentration with Alzheimer Disease Progression. *JAMA Neurology*, 1–8.
- Zetterberg, H., Skillbäck, T., Mattsson, N., Trojanowski, J. Q., Portelius, E., Shaw, L. M., et al. (2016). Association of Cerebrospinal Fluid Neurofilament Light Concentration with Alzheimer Disease Progression. *JAMA Neurology*, *73*(1), 60–67. doi:[10.1001/jamaneurol.2015.3037](https://doi.org/10.1001/jamaneurol.2015.3037).
- Zhang, H., Yushkevich, P. A., Alexander, D. C., & Gee, J. C. (2006). Deformable registration of diffusion tensor MR images with explicit orientation optimization. *Medical Image Analysis*, *10*(5), 764–785.
- Zhang, H., Avants, B. B., Yushkevich, P. A., Woo, J. H., Wang, S., McCluskey, L. F., et al. (2007). High-dimensional spatial normalization of diffusion tensor images improves the detection of white matter differences: An example study using amyotrophic lateral sclerosis. *Medical Imaging, IEEE Transactions on*, *26*(11), 1585–1597.
- Zhuang, L., Sachdev, P. S., Trollor, J. N., Reppermund, S., Kochan, N. A., Brodaty, H., et al. (2013). Microstructural white matter changes, not hippocampal atrophy, detect early amnesic mild cognitive impairment. *PloS One*, *8*(3), e58887.